PBHs and secondary GWs from ultra slow roll and punctuated inflation

H.V. Ragavendra

Department of Physics, IIT Madras, Chennai

November 12, 2020

based on the work, *H.V. Ragavendra, Pankaj Saha, L. Sriramkumar, and Joseph Silk arXiv:2008.12202 [astro-ph.CO].*

Overview

- Introduction
- Ultra slow roll and punctuated inflation
- Model reconstruction
- PBH production
- Secondary GWs
- Scalar bispectrum
- Secondary tensor bispectrum
- Summary

Introduction

- Ultra slow roll is a phase in inflation when the scalar field rolls with very small velocity. It may or may not be preceded by a brief interruption in inflation.
- Such ultra slow roll evolution can be achieved by having an inflection point in the potential describing the inflaton field.
- Models permitting ultra slow roll epoch are promising candidates to generate significant primordial black holes (PBHs) and associated secondary gravitational waves (SGWs).

Introduction

The scalar field driving inflation has the following equation of motion.

$$\ddot{\phi} + 3\,H\,\dot{\phi} + \frac{\mathrm{d}V}{\mathrm{d}\phi} = 0$$

The slow roll parameters that describe the dynamics of inflation are defined as[1]

$$\epsilon_1 \equiv -\frac{\mathrm{d}\,ln\,H}{\mathrm{d}N}\,, \quad \epsilon_{i+1} = \frac{\mathrm{d}\,ln\,\epsilon_i}{\mathrm{d}N}\,.$$

Slow roll approximation : $3\,H\,\dot{\phi} + \frac{\mathrm{d}V}{\mathrm{d}\phi} \simeq 0$, $\frac{\dot{\phi}^2}{2} < V(\phi)$.

$$\epsilon_1 \simeq \frac{M_{\rm Pl}^2}{2}\left(\frac{V_{,\phi}}{V}\right)^2, \quad \epsilon_2 \simeq 2M_{\rm Pl}^2\left[\left(\frac{V_{,\phi}}{V}\right)^2 - \frac{V_{,\phi\phi}}{V}\right].$$

Typically, $\epsilon_1 \lesssim \mathcal{O}(10^{-2})$, $\epsilon_{i+1} \sim \epsilon_1$. Inflation ends when $\epsilon_1 = 1$.

[1] e-fold $N \equiv ln(a/a_i)$, $H = \mathrm{d}ln\,a/\mathrm{d}t$, $M_{\rm Pl} = 1/\sqrt{8\pi G}$

Ultra slow roll and Punctuated inflation

In ultra slow roll or punctuated inflation, there is an inflection point in the potential.

$$\frac{\mathrm{d}V}{\mathrm{d}\phi} = 0\,, \quad \frac{\mathrm{d}^2V}{\mathrm{d}\phi^2} = 0\,.$$

The equation of motion around the inflection point is

$$\ddot{\phi} + 3\,H\,\dot{\phi} = 0\,.$$

In such a case,

$$\epsilon_1 \ll 1, \quad \epsilon_2 \simeq -\mathcal{O}(1)\ .$$

USR and PI

Ultra slow roll models:

- USR1 : $V(\phi) = V_0 \, \dfrac{6\,x^2 - 4\,\alpha\,x^3 + 3\,x^4}{(1+\beta\,x^2)^2}; \; x = \phi/v$
- USR2 : $V(\phi) = V_0 \, \left[x + A \, \sin\left(\dfrac{x}{f_\phi}\right)\right]^2; \; x = \tanh\left(\dfrac{\phi}{\sqrt{6}\,M_{\rm Pl}}\right)$

Punctuated inflationary models :

- PI1 : $V(\phi) = V_0 \, \left(1 + B\,\phi^4\right)$
- PI2 : $V(\phi) = \dfrac{m^2}{2}\,\phi^2 - \dfrac{2\,m^2}{3\,\phi_0}\,\phi^3 + \dfrac{m^2}{4\,\phi_0^2}\,\phi^4$
- PI3 : $V(\phi) = V_0 \, \left[c_0 + c_1\,x + c_2\,x^2 + c_3\,x^3\right]^2; \; x = \tanh\left(\dfrac{\phi}{\sqrt{6\,\alpha}}\right)$

USR and PI

Behavior of slow roll parameters is very similar between USR and PI models except at the peak of ϵ_1.
The ϵ_2 does not recover slow roll value after the ultra slow roll phase.

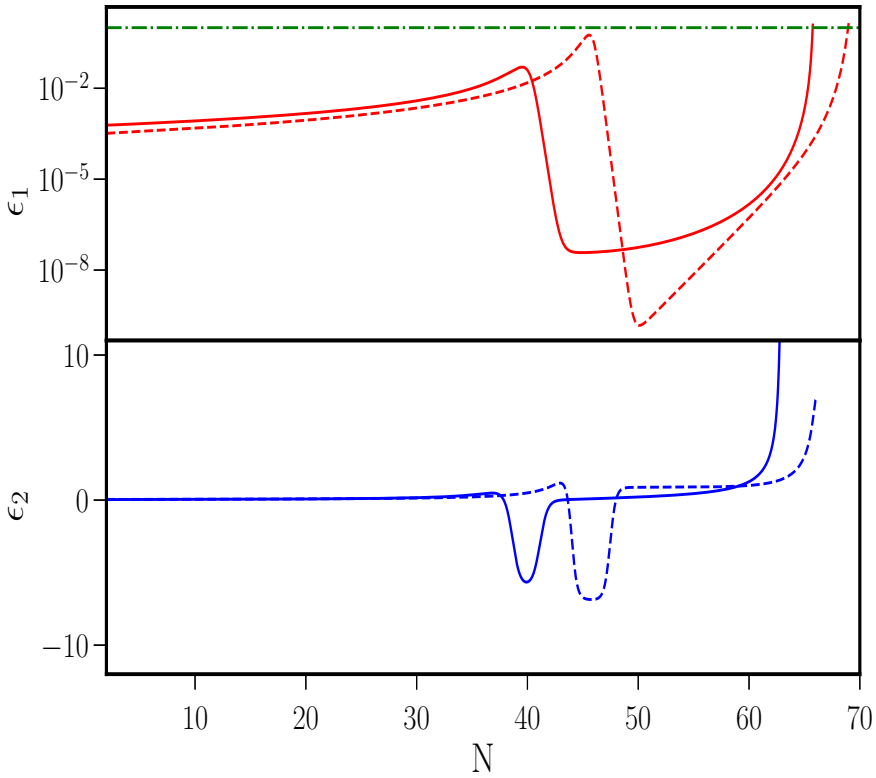

USR models

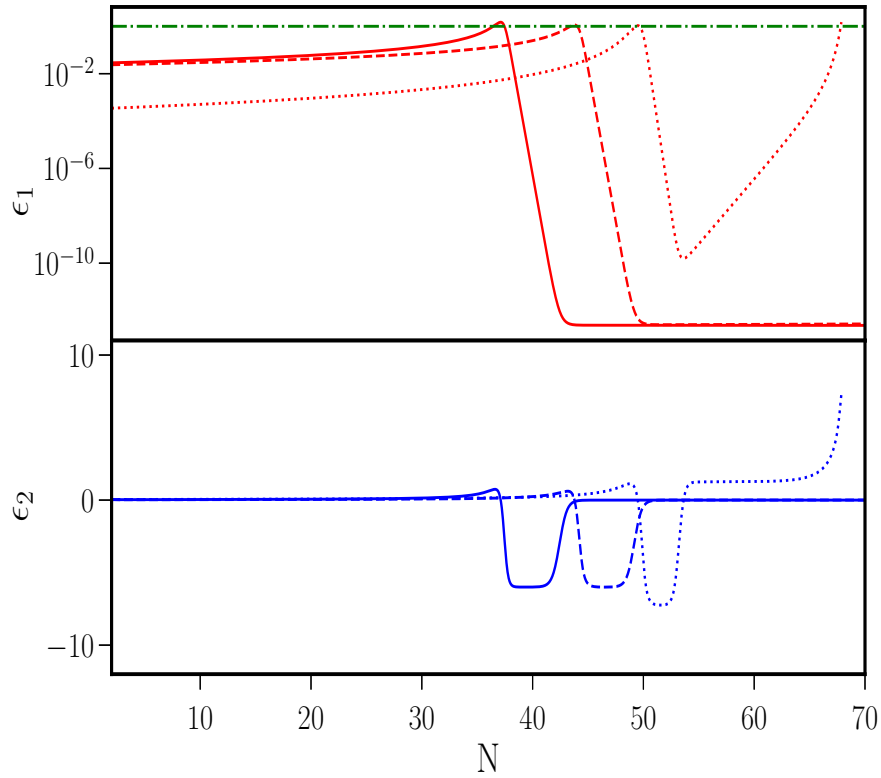

PI models

USR and PI - The power spectra

$$\mathcal{P}_{\mathcal{R}}(k) = k^3 \frac{|\mathcal{R}_k|^2}{2\pi^2} \simeq \frac{H^2}{8\pi^2\epsilon_1}\,, \quad \mathcal{P}_{\mathrm{T}}(k) = 4\,k^3 \frac{|h_k|^2}{2\pi^2} \simeq 2\,\frac{H^2}{\pi^2}\,.$$

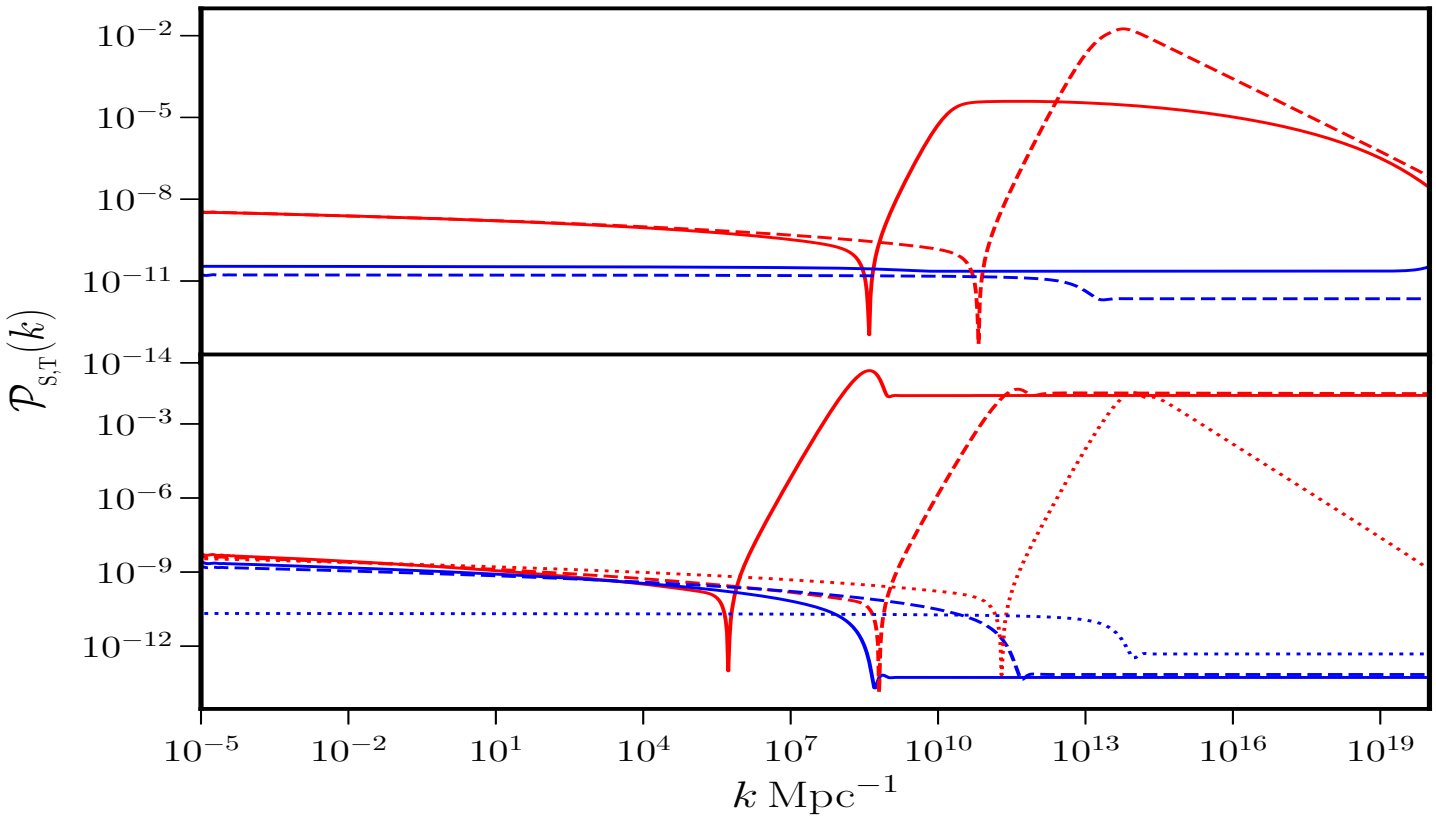

Scalar (red) and tensor (blue) power spectra from USR (top) and PI (bottom) models.

Model reconstruction

We reconstruct models of USR and PI using parametric forms of $\epsilon_1(N)$.

$$\text{RS1}: \quad \epsilon_1^{\rm I}(N) = [\epsilon_{1a}\ (1+\epsilon_{2a}\ N)]\left[1-\tanh\left(\frac{N-N_1}{\Delta N_1}\right)\right]+\epsilon_{1b}+\exp\left(\frac{N-N_2}{\Delta N_2}\right)$$

$$\text{RS2}: \quad \epsilon_1^{\rm II}(N) = \epsilon_1^{\rm I}(N)+\cosh^{-2}\left(\frac{N-N_1}{\Delta N_1}\right)$$

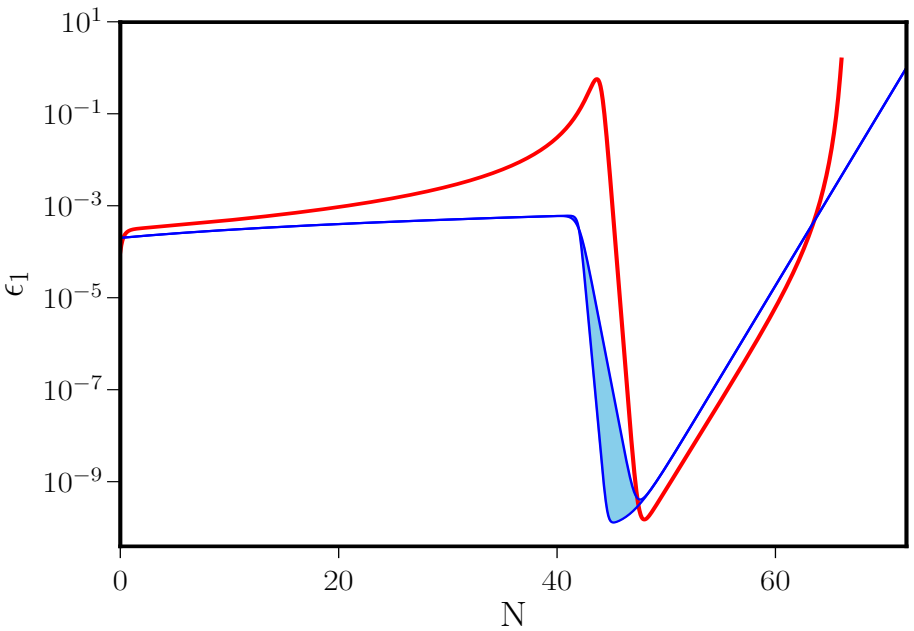

RS1 (blue) against USR2 (red)

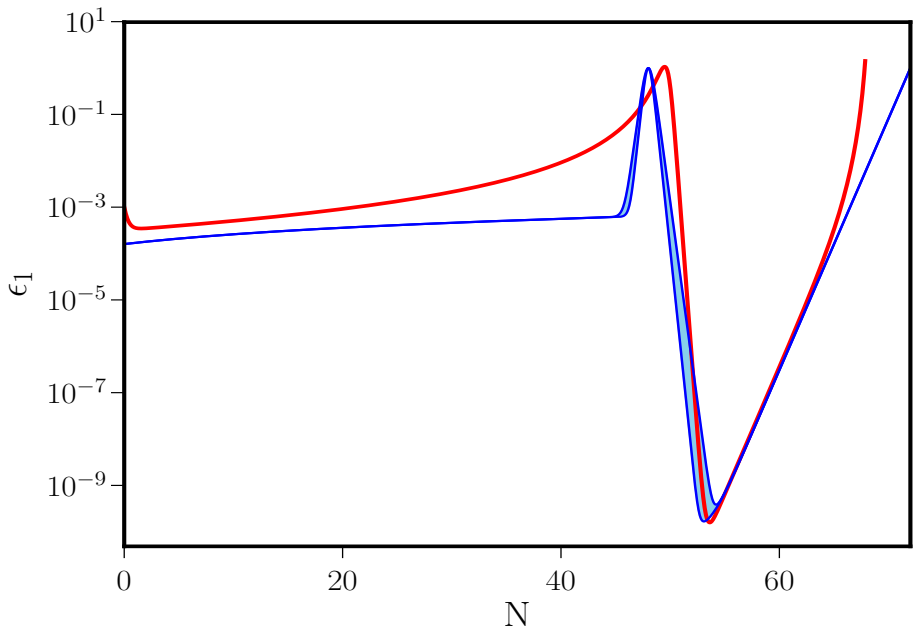

RS2 (blue) against PI3 (red)

Model reconstruction - potentials

We plot the potentials parametrically against the field evolution for the reconstructed $\epsilon_1(N)$.

$$\text{RS1}: \quad \epsilon_1^{\rm I}(N) = [\epsilon_{1a}\ (1+\epsilon_{2a}\ N)]\left[1-\tanh\left(\frac{N-N_1}{\Delta N_1}\right)\right]+\epsilon_{1b}+\exp\left(\frac{N-N_2}{\Delta N_2}\right)$$

$$\text{RS2}: \quad \epsilon_1^{\rm II}(N) = \epsilon_1^{\rm I}(N)+\cosh^{-2}\left(\frac{N-N_1}{\Delta N_1}\right)$$

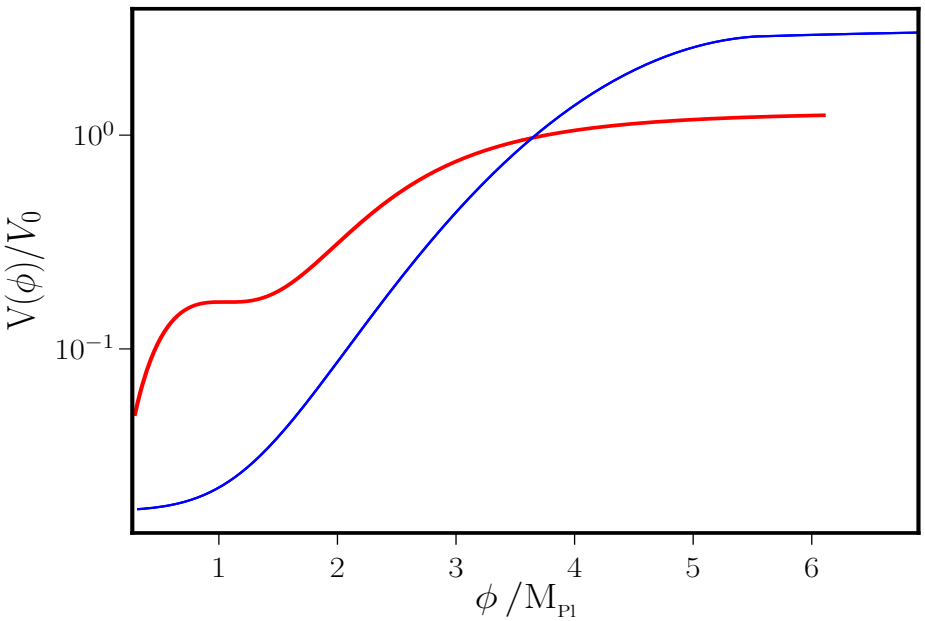

RS1 (blue) against USR2 (red)

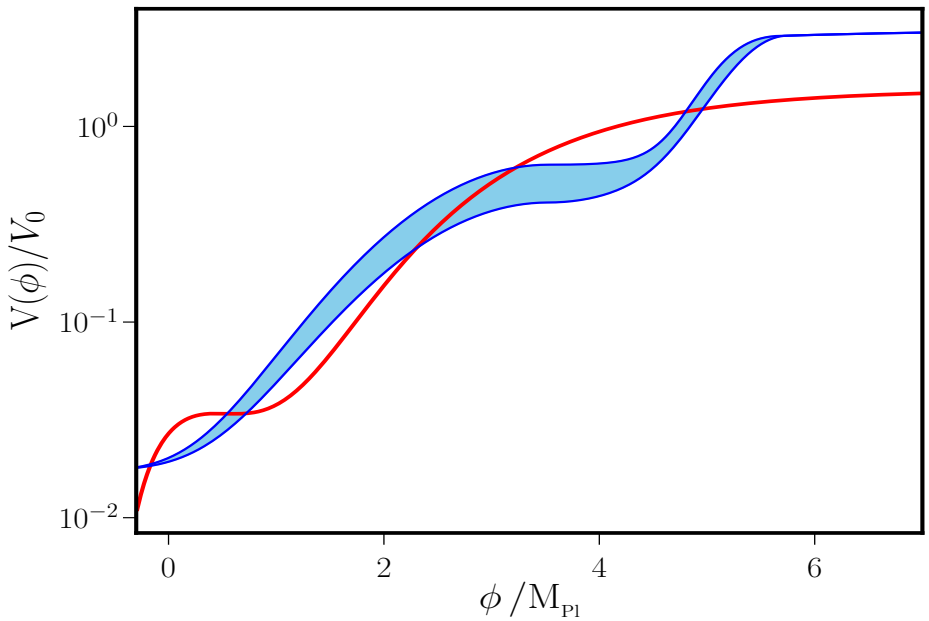

RS2 (blue) against PI3 (red)

Model reconstruction - power spectra

We vary N_1 to produce peaks at different scales and ΔN_1 to determine the height of the peak.

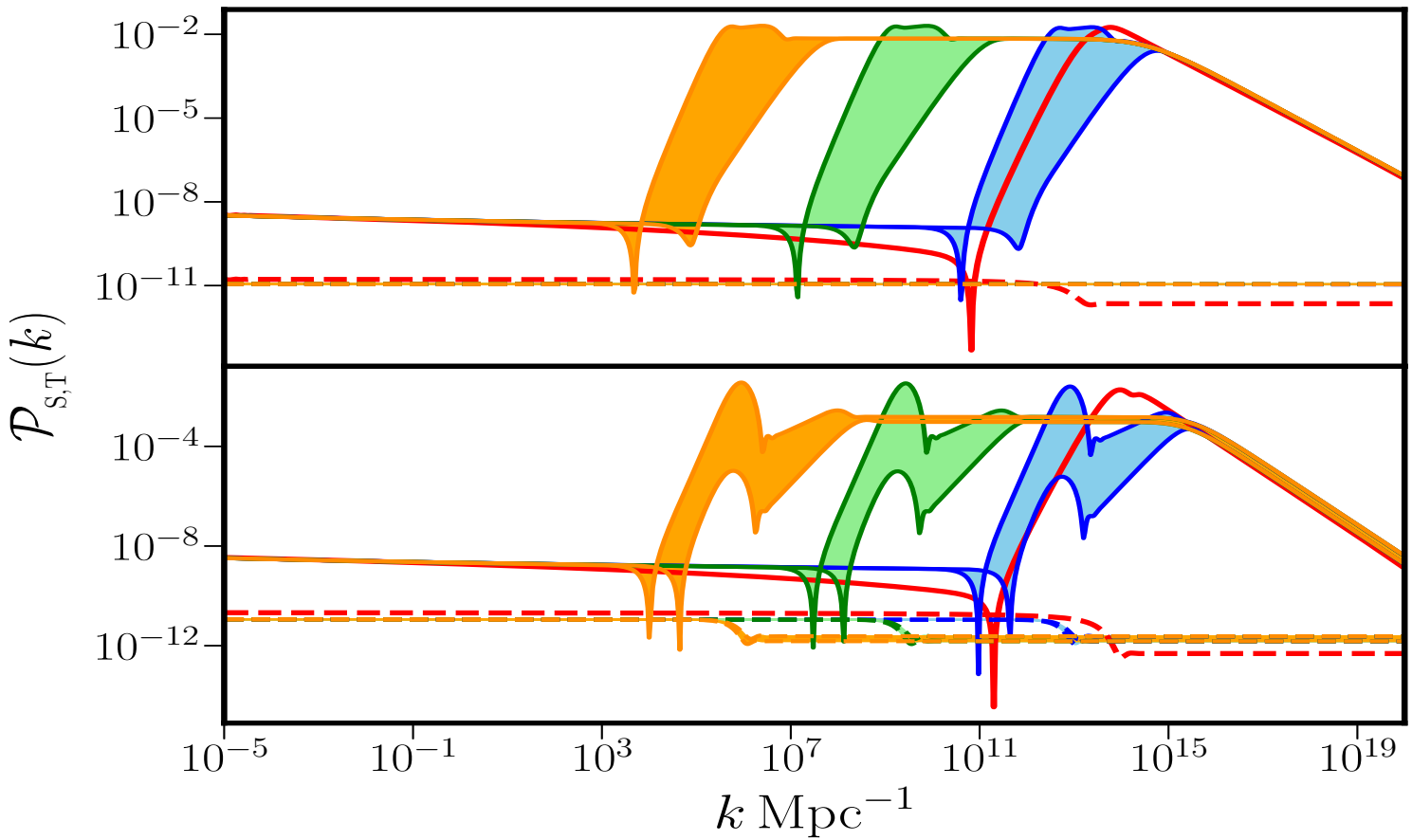

Scalar and tensor power spectra from RS1 (top) and RS2 (bottom) models.

PBH production in USR and PI

$$f_{\rm PBH}(M) = 2^{1/4}\,\gamma^{3/2}\,\beta(M)\left(\frac{\Omega_{\rm m}\,h^2}{\Omega_{\rm c}\,h^2}\right)\left(\frac{g_{*,k}}{g_{*,\rm eq}}\right)^{-1/4}\left(\frac{M}{M_{\rm eq}}\right)^{-1/2}$$

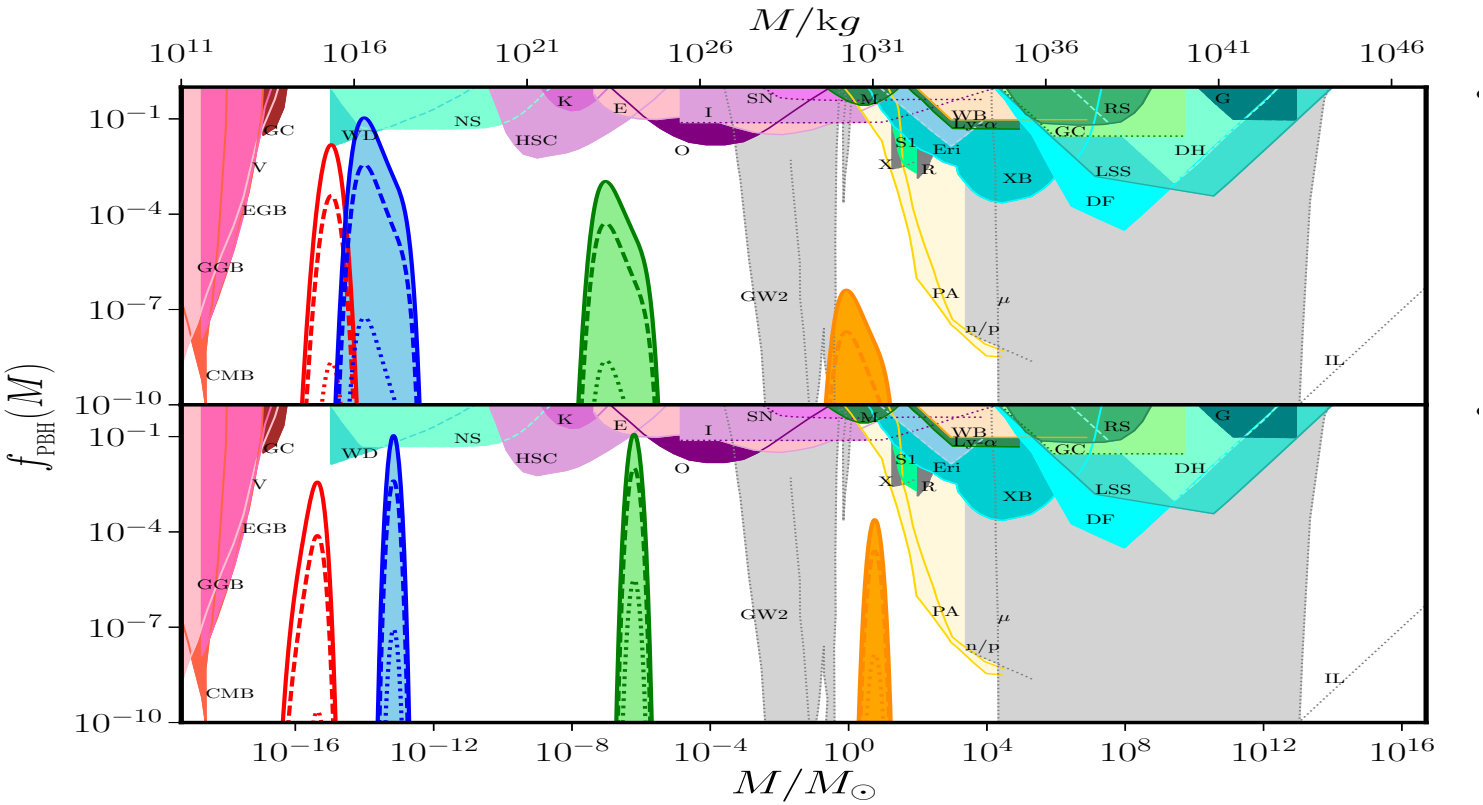

$f_{\rm PBH}$ from USR2 and PI3 models and reconstructions of RS1 and RS2.

see, for instance, B. Carr et al., arXiv:2002.12778 [astro-ph.CO]

Secondary GWs from USR and PI

$$h^2\,\Omega_{\rm GW}(k) = \left(\frac{g_{*,k}}{g_{*,0}}\right)^{-1/3} \Omega_{\rm r}\,h^2\,\Omega_{\rm GW}(k,\eta)$$

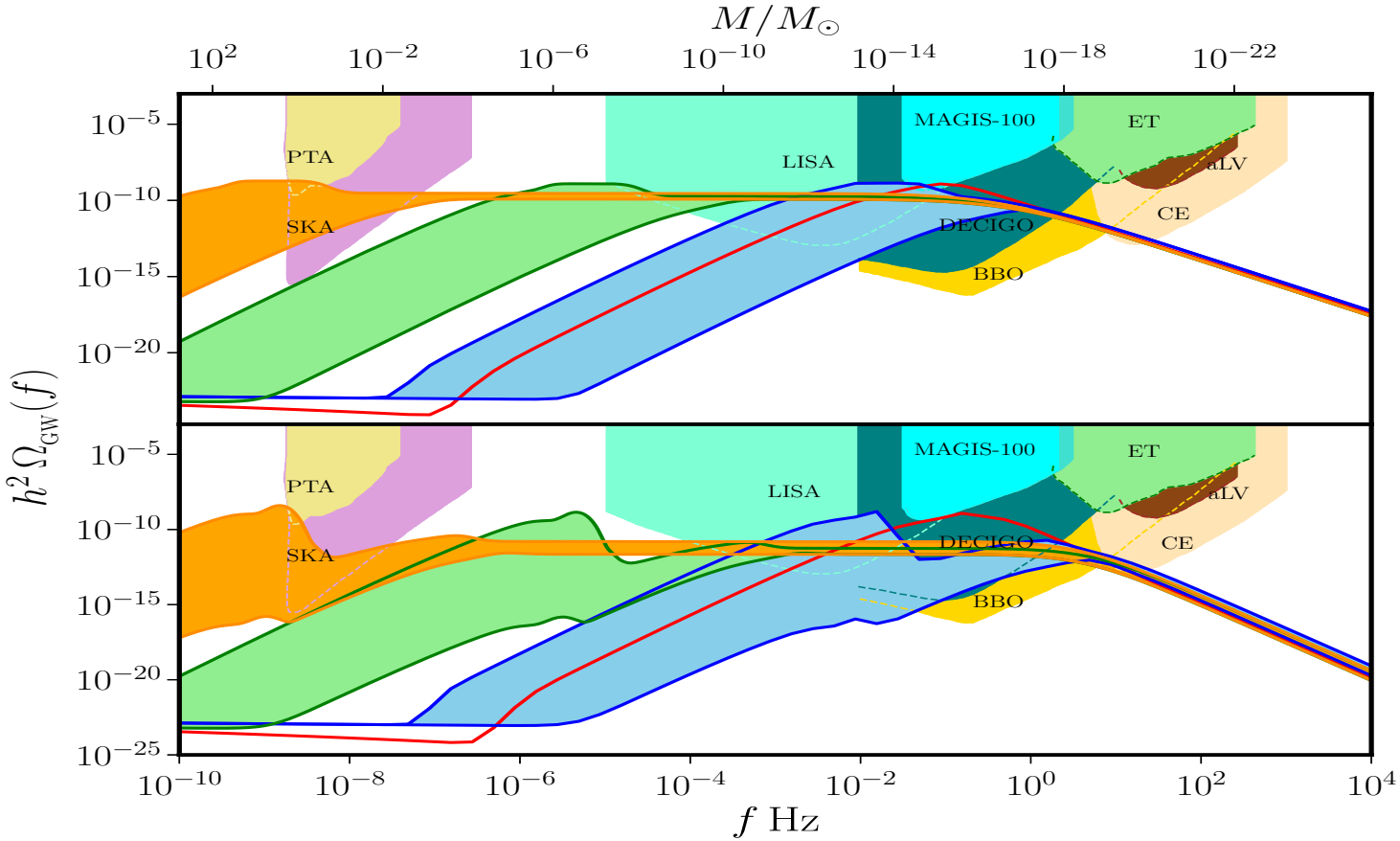

$\Omega_{\rm GW}$ from USR2 and PI3 models and reconstructions of RS1 and RS2.

---

see, for instance, N. Bartolo et al., Phys. Rev. D **99**, *103521 (2019);*
C. .J. Moore et al., Class. Quant. Grav. **32**, *015014 (2015).*

Scalar bispectrum

We compute the effect of of scalar bispectrum on $f_{\rm PBH}$ and $\Omega_{\rm GW}$.

$$\mathcal{R}(\eta, \boldsymbol{x}) = \mathcal{R}^{\rm G}(\eta, \boldsymbol{x}) - \frac{3}{5} f_{\rm NL} \left[\mathcal{R}^{\rm G}(\eta, \boldsymbol{x})\right]^2 .$$

Using this $f_{\rm NL}$ we compute the correction to the scalar power spectrum.

$$\langle \hat{\mathcal{R}}_{\boldsymbol{k}} \hat{\mathcal{R}}_{\boldsymbol{k}'} \rangle = \frac{2\pi^2}{k^3} \delta^{(3)}(\boldsymbol{k} + \boldsymbol{k}') \left[\mathcal{P}_{\mathcal{R}}(k) + \left(\frac{3}{5}\right)^2 \frac{k^3}{2\pi} f_{\rm NL}^2 \int {\rm d}^3\boldsymbol{p} \, \frac{\mathcal{P}_{\mathcal{R}}(p)}{p^3} \, \frac{\mathcal{P}_{\mathcal{R}}(|\boldsymbol{k} - \boldsymbol{p}|)}{|\boldsymbol{k} - \boldsymbol{p}|^3}\right] .$$

Thus the correction to the spectrum $\mathcal{P}_{\rm C}(k)$ is

$$\mathcal{P}_{\rm C}(k) = \left(\frac{3}{5}\right)^2 f_{\rm NL}^2 \int_0^\infty {\rm d}v \int_{|1-v|}^{1+v} \frac{{\rm d}u}{u^2 v^2} \, \mathcal{P}_{\mathcal{R}}(k\,v) \, \mathcal{P}_{\mathcal{R}}(k\,u) .$$

R-G. Cai et al., Phys. Rev. Lett. **122**, *201101 (2019);*
C. Unal, Phys. Rev. D **99**, *041301 (2019).*

Scalar bispectrum

We calculate the scalar bispectrum $G(\boldsymbol{k}_1, \boldsymbol{k}_2, \boldsymbol{k}_3)$ in two limits - equilateral $(k_1 = k_2 = k_3)$ and squeezed $(\boldsymbol{k}_1 = \boldsymbol{0},\ \boldsymbol{k}_2 = -\boldsymbol{k}_3)$.

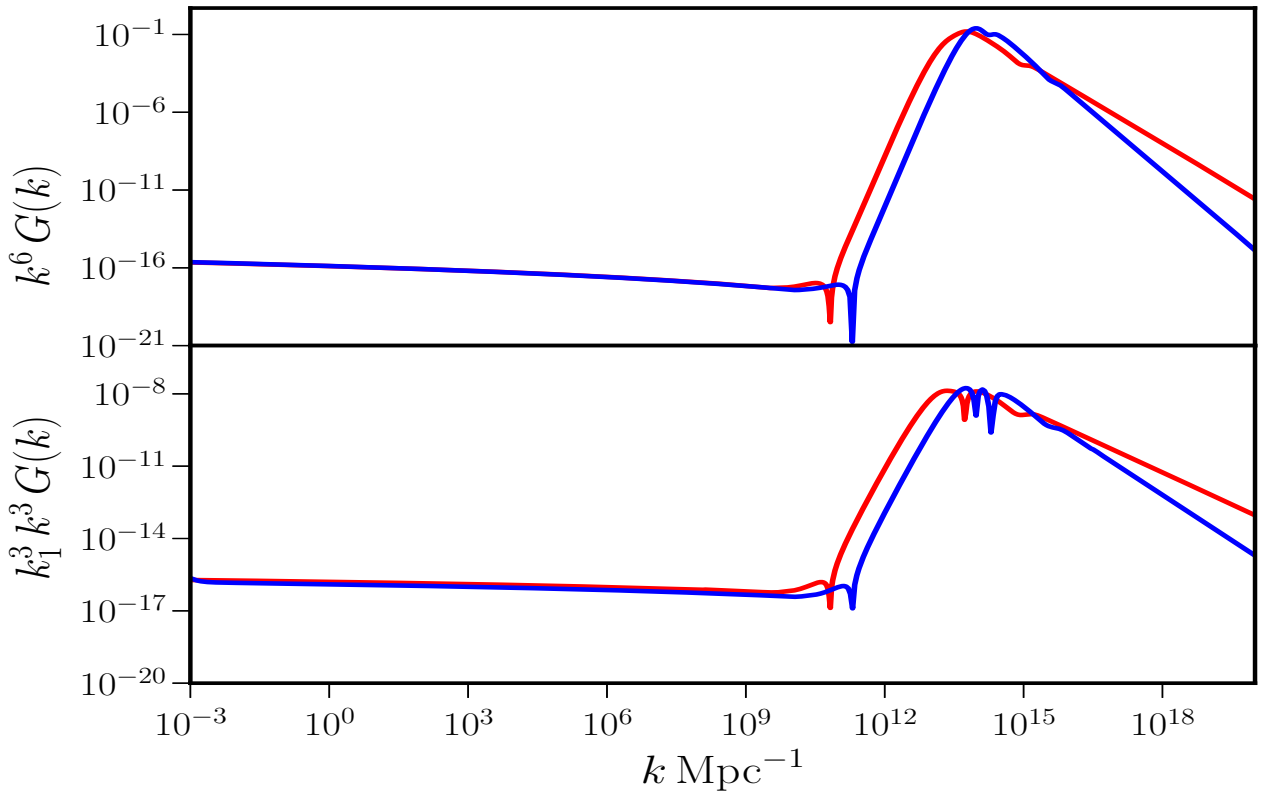

USR2 (red) and PI3 (blue) in
equilateral limit (top) and squeezed limit (bottom)

Scalar bispectrum - $f_{\rm NL}$ in USR

$$f_{\rm NL}(\boldsymbol{k}_1, \boldsymbol{k}_2, \boldsymbol{k}_3) = -\frac{10}{3}\,\frac{1}{(2\,\pi)^4}\,k_1^3\,k_2^3\,k_3^3\,G(\boldsymbol{k}_1, \boldsymbol{k}_2, \boldsymbol{k}_3)\Big[k_1^3\,\mathcal{P}_{\mathcal{R}}(k_2)\,\mathcal{P}_{\mathcal{R}}(k_3) + \text{two permutations}\Big]^{-1}\,.$$

In the squeezed limit, $f_{\rm NL} = 5(n_{\rm S} - 1)/12$.

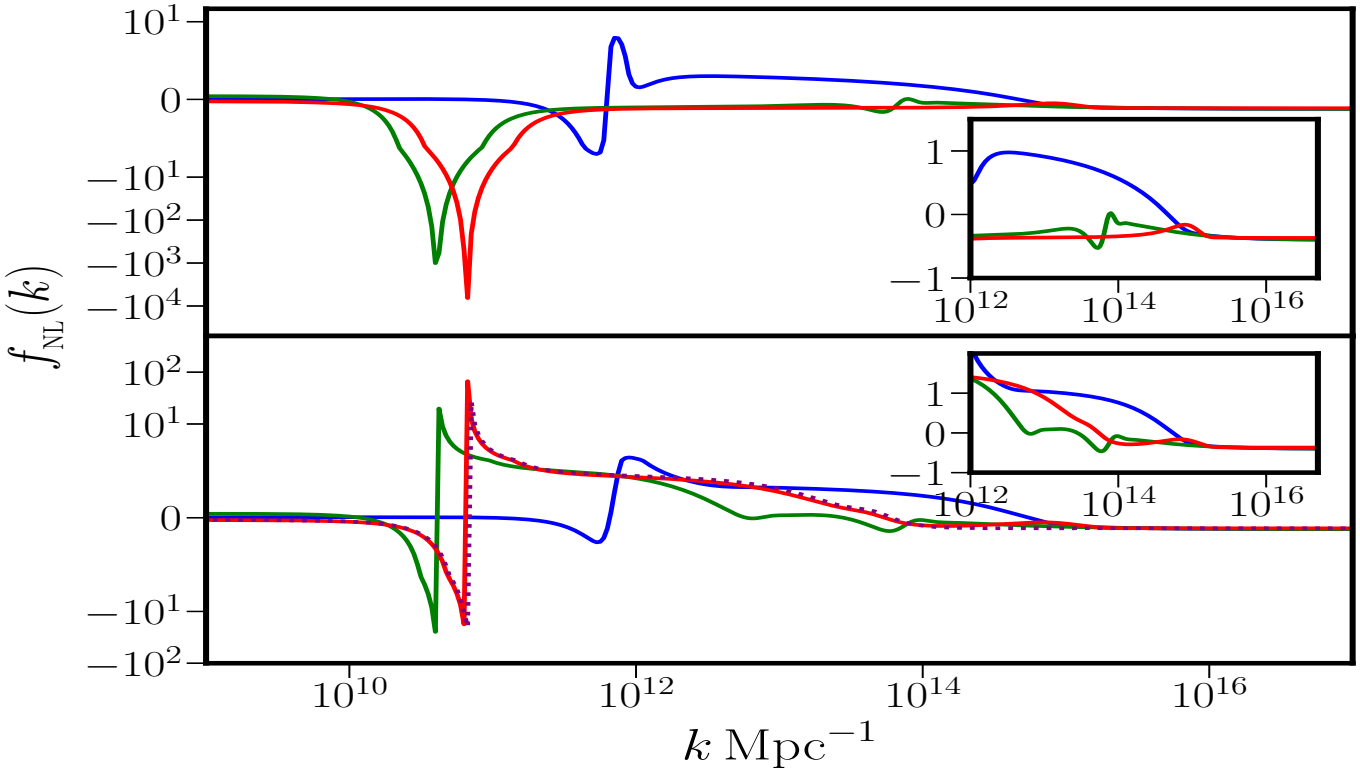

USR2 (red) and RS1 (blue and green)
equilateral limit (top) and squeezed limit (bottom)

$n_{\rm S} - 1 = {\rm d}ln\mathcal{P}_{\mathcal{R}}/{\rm d}lnk$, the scalar spectral index.

Scalar bispectrum - Effect on PBHs and GWs

$$\mathcal{P}_{\rm C}(k) = \left(\frac{3}{5}\right)^2 f^2_{\rm NL}(k) \int_0^\infty {\rm d}v \int_{|1-v|}^{1+v} \frac{{\rm d}u}{u^2\, v^2}\, \mathcal{P}_{\mathcal{R}}(k\, v)\, \mathcal{P}_{\mathcal{R}}(k\, u)\,.$$

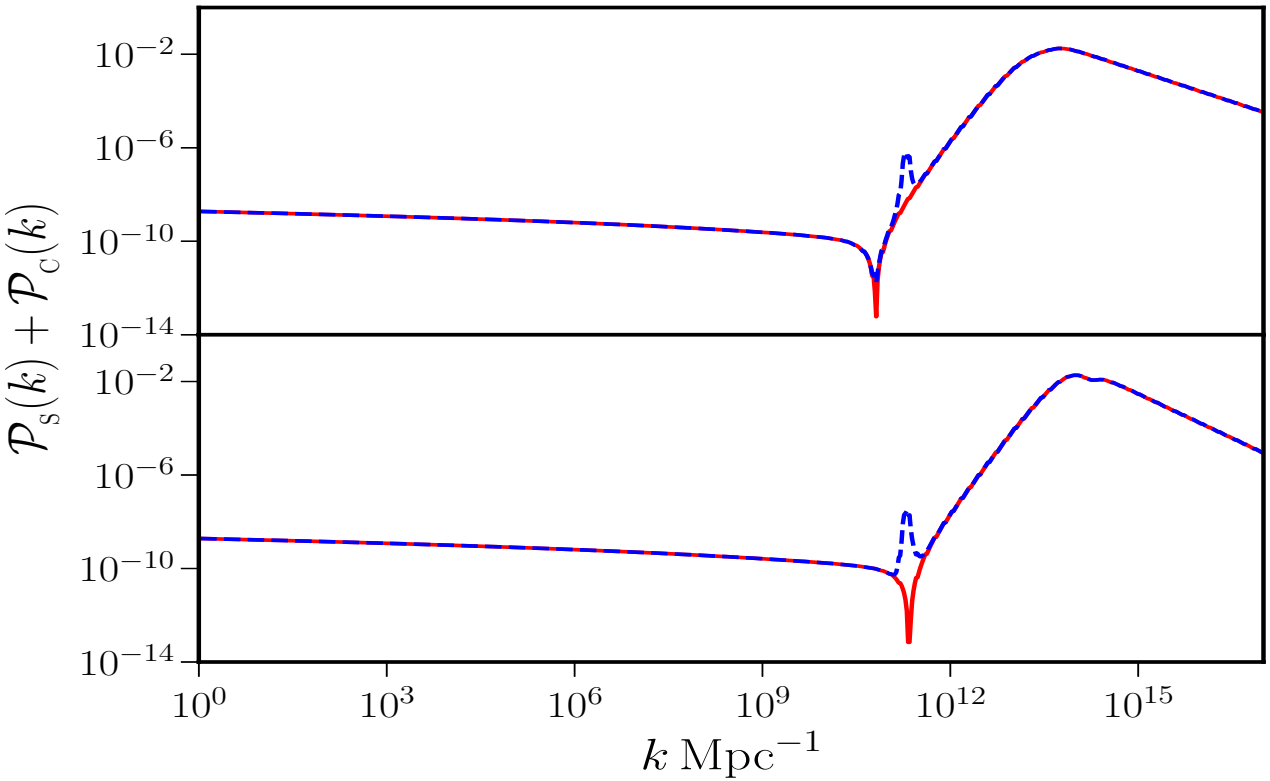

The scalar power spectrum and the non-Gaussian correction for USR2 (top) and PI3 (bottom)

Secondary tensor bispectrum

The secondary tensor bispectrum, say, $G_h^{\lambda_1\lambda_2\lambda_3}(\boldsymbol{k}_1, \boldsymbol{k}_2, \boldsymbol{k}_3)$ is defined as[1]

$$\left\langle h_{\boldsymbol{k}_1}^{\lambda_1}(\eta)\, h_{\boldsymbol{k}_2}^{\lambda_2}(\eta)\, h_{\boldsymbol{k}_3}^{\lambda_3}(\eta) \right\rangle = (2\,\pi)^{15/2}\, G_h^{\lambda_1\lambda_2\lambda_3}(\boldsymbol{k}_1, \boldsymbol{k}_2, \boldsymbol{k}_3, \eta)\, \delta^{(3)}(\boldsymbol{k}_1 + \boldsymbol{k}_2 + \boldsymbol{k}_3)\,,$$

where $\lambda = [+, \times]$ denotes the polarization of $h_{\boldsymbol{k}}$.

Only two combinations $G_h^{+++}(k)$, $G_h^{+\times\times}(k)$ are unique and non-zero in the equilateral limit.

We compute and the associated shape function $S_h^{\lambda_1\lambda_2\lambda_3}(k)$ which is defined as

$$S_h^{\lambda_1\lambda_2\lambda_3}(k) = \frac{k^6\, G_h^{\lambda_1\lambda_2\lambda_3}(k, \eta)}{\sqrt{\mathcal{P}_h^3(k, \eta)}}.$$

[1] *N. Bartolo et al., JCAP* **12**, *026 (2016).*

Secondary tensor bispectrum

$$S_h^{\lambda_1\lambda_2\lambda_3}(k) = \frac{k^6\, G_h^{\lambda_1\lambda_2\lambda_3}(k,\eta)}{\sqrt{\mathcal{P}_h^3(k,\eta)}}.$$

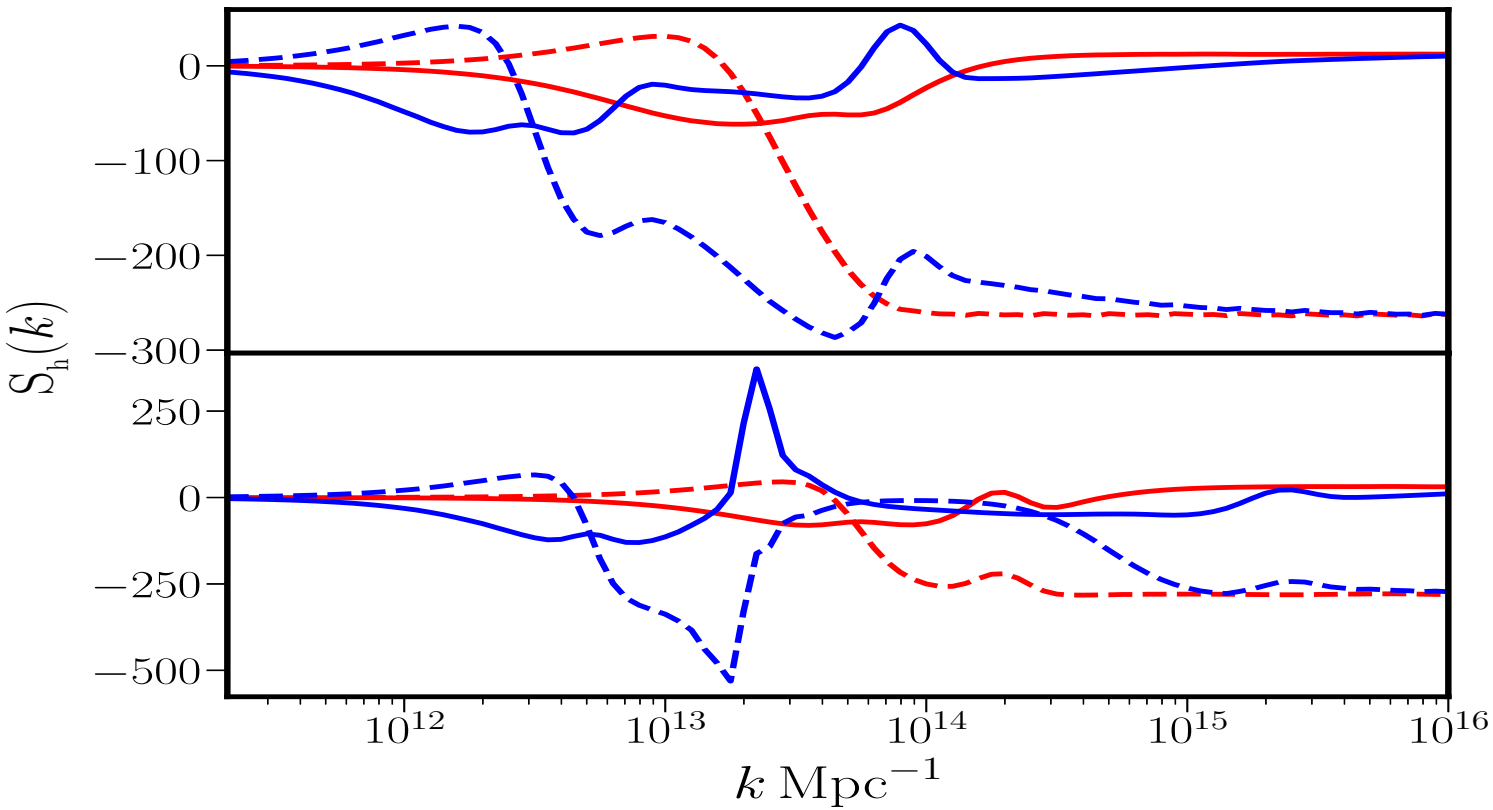

$S_h(k)$ in the equilateral limit for the models
USR2 (red), RS1 (blue) on the top and PI3 (red), RS2 (blue) in the bottom,
for $(+++)$ (in solid lines) and $(+\times\times)$ (in dashed lines) configurations.

Summary

- USR and PI models are the most promising candidates among models for generating PBHs and secondary GWs.
- Reconstruction of ϵ_1 with USR behavior provides insight about the dynamics and helps in easy constraining of these models.
- The consistency condition is satisfied despite strong features in the scalar power and bi-spectra. Hence there are no significant corrections to the power spectra.
- The secondary tensor bispectrum has unique features that may help in better constraining of these models against future datasets.

Summary

- USR and PI models are the most promising candidates among models for generating PBHs and secondary GWs.
- Reconstruction of ϵ_1 with USR behavior provides insight about the dynamics and helps in easy constraining of these models.
- The consistency condition is satisfied despite strong features in the scalar power and bi-spectra. Hence there are no significant corrections to the power spectra.
- The secondary tensor bispectrum has unique features that may help in better constraining of these models against future datasets.

Thank you for your attention.